

Photocatalytic (Hetero)Arylation of C(sp³)–H Bonds with Carbon Nitride

Saikat Das¹, Kathiravan Murugesan¹, Gonzalo J. Villegas Rodríguez¹, Jaspreet Kaur¹, Joshua P. Barham¹, Aleksandr Savateev², Markus Antonietti² and Burkhard König^{1*}

¹Fakultät für Chemie und Pharmazie, Universität Regensburg, 93040 Regensburg, Germany

²Department of Colloid Chemistry, Max-Planck Institute of Colloids and Interfaces, Research Campus Golm, 14424 Potsdam, Germany

*Correspondence: burkhard.koenig@ur.de

Abstract

Polymeric graphitic carbon nitride materials have attracted significant interest in recent years and found applications in diverse light-to-energy conversions such as artificial photosynthesis, CO₂ reduction or degradation of organic pollutants. However, their utilization in synthetic photocatalysis especially in the direct functionalization of C(sp³)–H bonds remains underexplored. Herein, we report mesoporous graphitic carbon nitride (mpg-CN) as a heterogeneous organic semiconductor photocatalyst for direct arylation of sp³ C–H bonds *via* a combination of hydrogen atom transfer and nickel catalysis. Our protocol has a broad synthetic scope (>70 examples including late-stage modification of densely functionalized bio-active molecules), is operationally simple, and shows high chemo- and regioselectivity. Facile separation and recycling of the mpg-CN catalyst in combination with its low preparation cost, innate photochemical stability and low toxicity are beneficial features overcoming typical shortcomings of homogeneous photocatalysis. Additionally, mechanistic investigations indicate that an unprecedented energy transfer process (EnT) from the organic semiconductor to the nickel complex is operating.

Over the last decade, the use of visible light has had a resurgence as an ideal reagent for catalytic synthetic transformations¹. It is non-toxic, abundant, generates no waste, and acts as ‘traceless reagent’ even when used in excess. Importantly, it can be selectively transferred to substrates by photocatalysts via electron, hole or energy transfer processes. Where visible light is a fundamental energy source powering biological photosynthesis in nature, chemists harness visible light to increase the efficiency of synthesis and realize new reaction pathways^{2,3}. A recent application of visible light photocatalysis is the direct functionalization of C(sp³)-H bonds. Since such bonds are the most abundant moiety in organic molecules, their direct activation allows for efficient chemical diversification avoiding pre-functionalization steps^{4,5}. Specially designed homogeneous catalysts such as transition metal based polypyridine complexes⁶ or organic dyes⁷ and in some cases inorganic semiconductors⁸ have been used for C-H bond functionalization. However, in practice, most solution-phase catalysts show limited durability; they are prone to deactivation in the presence of reactive radical intermediates^{7,9-11} or suffer from drastic changes to their photophysical properties upon changes in the pH of the reaction medium¹². The selection of a photocatalyst for a given transformation therefore remains a challenge. In addition to catalyst instability, the non-recyclability limits the practical use of many well-known homogeneous catalysts for direct functionalization of C-H bonds, particularly on a larger scale. Herein, we report the use of a heterogeneous organic semiconductor, mesoporous graphitic carbon nitride (mpg-CN), as a robust photocatalyst for direct arylations of C(sp³)-H bonds.

Graphitic carbon nitride, the most stable allotrope of carbon nitride, is a purely organic semiconductor material composed of the earth-abundant light elements carbon and nitrogen^{13,14}. One of its morphology-wise modified analogues, called mesoporous graphitic carbon nitride (mpg-CN), is especially attractive as a heterogeneous catalyst due to its larger surface area, more active sites and enhanced light harvesting capacity. Even though its first synthesis dates back to 1834¹⁵, mpg-CN and its congeners have only recently been recognized as photocatalysts for synthetic applications¹⁶. This polymeric material possesses suitable valence band maxima (VBM) and conduction band minima (CBM), spanning a band gap of approximately 2.7 eV upon visible light photoexcitation. Such a powerful redox window is not only equal or even wider than many commonly used photocatalysts (**Fig. 1b**), but it is also well-balanced for controlled oxidation and reduction of substrates. Although mpg-CN is yet to be commercialized, the cost of its synthesis falls within the range of a few euros/kg due to its inexpensive synthetic precursors (*e.g.*, urea and melamine) and easy synthetic procedures (see the Supplementary Methods)¹⁷. Owing to its outstanding thermal, chemical and photostability,

mpg-CN has found applications (**Fig. 1a**) mainly in hydrogen production by overall water splitting¹³ and carbon dioxide reduction^{18,19} as well as in several synthetic transformations¹⁶. Surprisingly, mpg-CN has rarely been used as a photocatalyst for direct C(sp³)-H functionalization by hydrogen atom transfer (HAT) chemistry^{20,21}. The synergistic combination of homogeneous photocatalysis, HAT and transition metal catalysis has provided several methods for selective C-H bond functionalization²²⁻²⁴, most of which remain restricted to either the use of i) activated Michael acceptors (electron-deficient olefins)²⁵⁻²⁷ or ii) stoichiometric

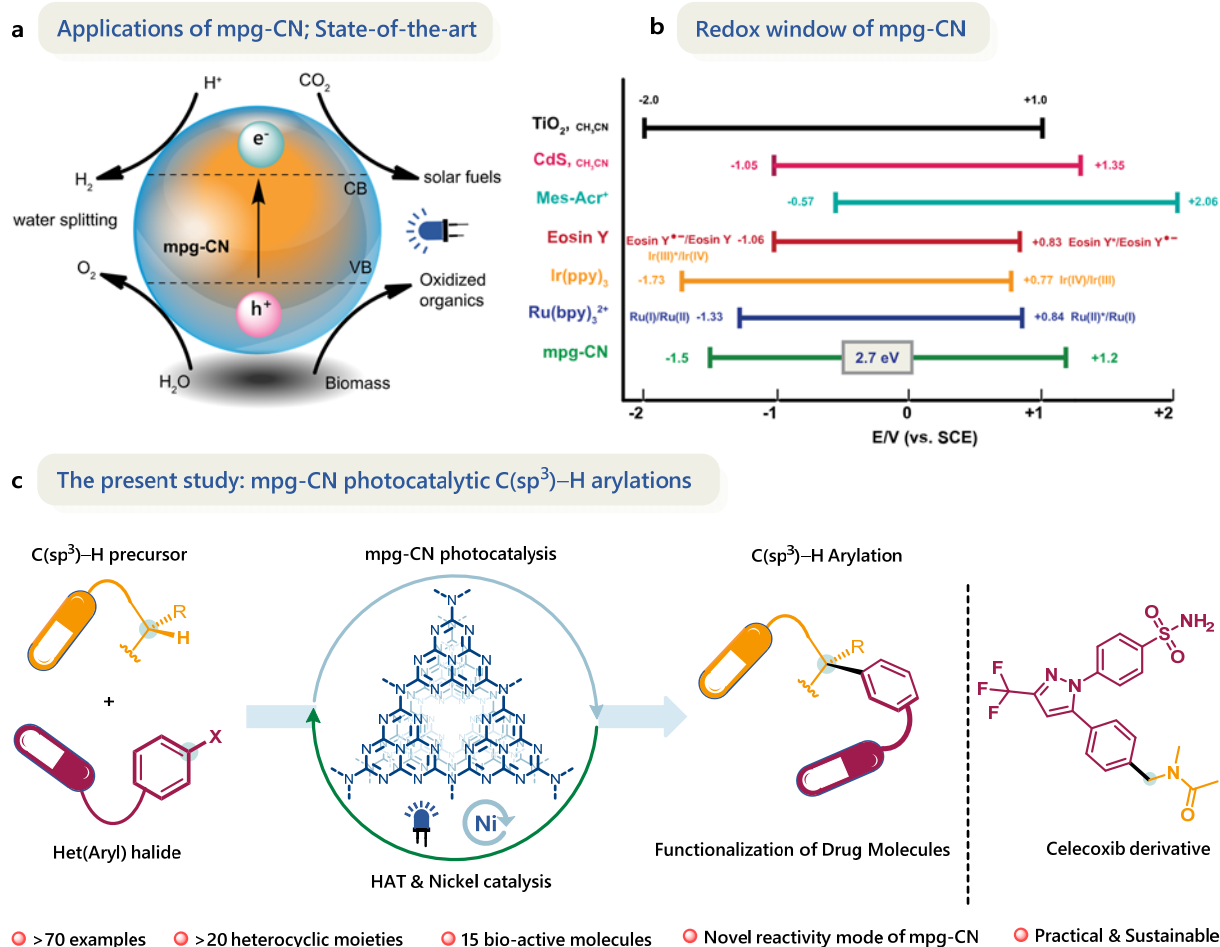
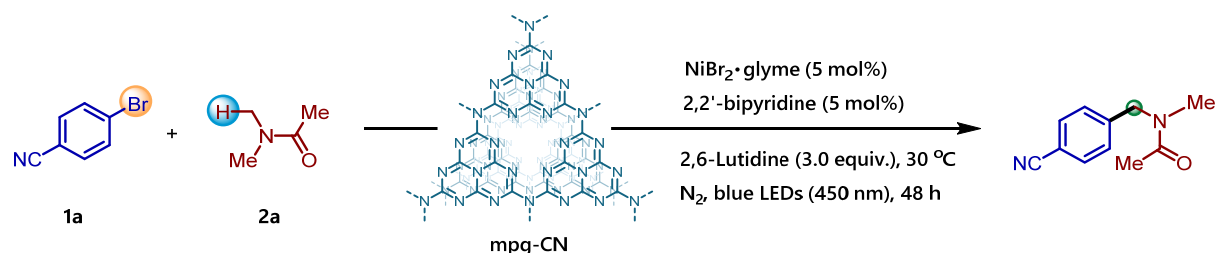


Fig. 1 | Schematic representation of photocatalytic reactivity of mpg-CN.

amount of HAT agents²⁸. Taking lessons from free radical halogenation chemistry of alkanes, we anticipated that the catalytically-formed halogen radicals on the mpg-CN surface might involve in a HAT event for the generation of carbon radicals, which in combination with transition metal catalysis would enable arylation of C(sp³)-H bonds with aryl halides (**Fig. 1c**). Herein, we describe mpg-CN photocatalytic arylation of C(sp³)-H bonds in combination with nickel as metal catalyst; as a robust, practical and tolerant protocol even suitable for late-stage functionalization of bio-active molecules. The reaction is selective for C-H activations α -to amide groups. Mechanistic investigations suggest energy transfer (EnT) from the organic

Table 1 | Selected optimization and control experiments for mpg-CN photocatalyzed C(sp³)-H bond arylation



Entry	Deviation from standard conditions ^a	Yield (%) ^b
1.	none	90(85)^c
2.	no mpg-CN	ND
3.	no NiBr ₂ ·glyme	ND
4.	no light	ND
5.	no ligand	<5
6.	no 2,6-lutidine	11
7.	no [Ni] catalyst & recovered mpg-CN	ND
8.	dtbbpy instead of bpy	52
9.	K ₃ PO ₄ instead of 2,6-lutidine	13
10.	no degassing and under N ₂	74
11.	under air	59
12.	NiBr ₂ ·3H ₂ O instead of NiBr ₂ ·glyme	72

^aReaction Conditions: 4-bromobenzonitrile (36.4 mg, 0.2 mmol), mpg-CN(10 mg), NiBr₂·glyme (3.2 mg, 5.0 mol%), 2,2'-bipyridine (1.6 mg, 5.0 mol%), 2,6-lutidine (70 μL, 3.0 equiv.) in 1 mL DMA under blue light irradiation (450±15 nm) at 30 °C for 48 h. ^bYields were determined by GC-FID using 1,4-dimethoxybenzene as an internal standard. ^cYield of isolated product. ND, not detected.

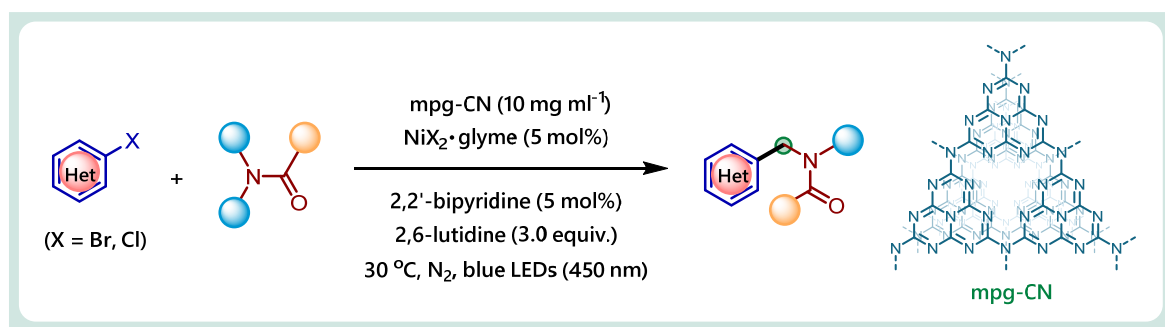
semiconductor to the nickel metal centre as a new reaction mode distinguishing this reaction from typical semiconductor single electron transfer (SET). The synergistic use of HAT and EnT²⁹ as mediated *via* a heterogeneous semiconductor photocatalyst is a concept expected to greatly expand the boundaries of synthetic photocatalysis.

Results

Reaction development. We focused our investigation on the activation of C(sp³)-H bond adjacent to the nitrogen atom of amides due to the importance of this functional group. Particularly, benzyl amines with *N*-electron withdrawing groups are a prominent substructure in drugs, such as compounds for the treatment of plaque psoriasis, seizures or diabetes³⁰. In a

typical synthesis, they are prepared through alkylation of amides with benzyl halides, but the chemical diversity of commercially available benzyl halides is limited. In contrast, the direct C–H arylation α -to amide *N*-atom constitutes a potentially better approach considering the available large number of aryl halides in chemical feedstocks, drug molecules and natural products. As a model system, 4-bromobenzonitrile was employed towards the C(sp³)–H bond arylation of *N,N*-dimethyl acetamide (DMA) as both C–H precursor and solvent. **Table 1** summarizes the optimization of the reaction parameters and control experiments (see the Supplementary Information for additional data). After systematic evaluation of various nickel(II) salts, ligands and bases, we found that a mixture consisting of NiBr₂·glyme, 2,2'-bipyridine, 2,6-lutidine and mpg-CN under blue LED (450±15 nm) irradiation at ambient temperature furnished the best result for our desired transformation, obtaining **1a** in 85% isolated yield after 48 h (**Table 1**, entry 1). The dehalogenation of starting material (benzonitrile) was the only detectable side product of the reaction. The reaction only required simple mixing of all the components in a vial followed by photoillumination. Control experiments which are either performed without mpg-CN, [Ni] catalyst, light or ligand revealed the necessity of each component for this novel C–C bond forming reaction (entries 2-5). Curiously, even in the absence of 2,6-lutidine, the reaction proceeded to some extent, possibly due to the basic nature of the bipyridine ligand (entry 6). The employment of recycled mpg-CN, without the renewed addition of [Ni] catalyst failed to afford the reaction product, corroborating the absence of active nickel catalyst remaining on the surface of the heterogeneous photocatalyst (entry 7). Unsubstituted bipyridine (bpy) served as the optimal ligand system; which is cheaper than dtbbpy (4,4'-di-*tert*-butyl 2,2'-bipyridine), the most commonly employed ligand in metallaphotoredox chemistry (entry 8). The choice of base is a crucial parameter, since most of the commonly employed inorganic or organic bases were ineffective in the reaction (entry 9 and Table S3). Ultimately, the use of 2,6-lutidine as a base proved to be optimal for this transformation. Comparable yields were also obtained without degassed solvents or under air (entries 10 and 11) or with inexpensive NiBr₂·3H₂O as nickel source (entry 12), thus showcasing the robustness of the mpg-CN photocatalytic C(sp³)–H bond arylation method.

Scope of our protocol. With the optimized reaction conditions in hand, we next explored the scope of the mpg-CN/nickel catalyzed arylation process. Initially we examined, the generality of aryl halides as partners. As evident from the examples listed in **Fig. 2a**, a diverse multitude of aryl halides bearing either electron-donating or electron-withdrawing substituents underwent C(sp³)–H arylation with DMA. Notably, mpg-CN photocatalytic C–H arylation displayed an excellent chemo-selectivity profile. For example, nitrile (**1a**), ester (**2**), ketone (**3**), aldehyde (**4**),



Scope of Aryl Halides

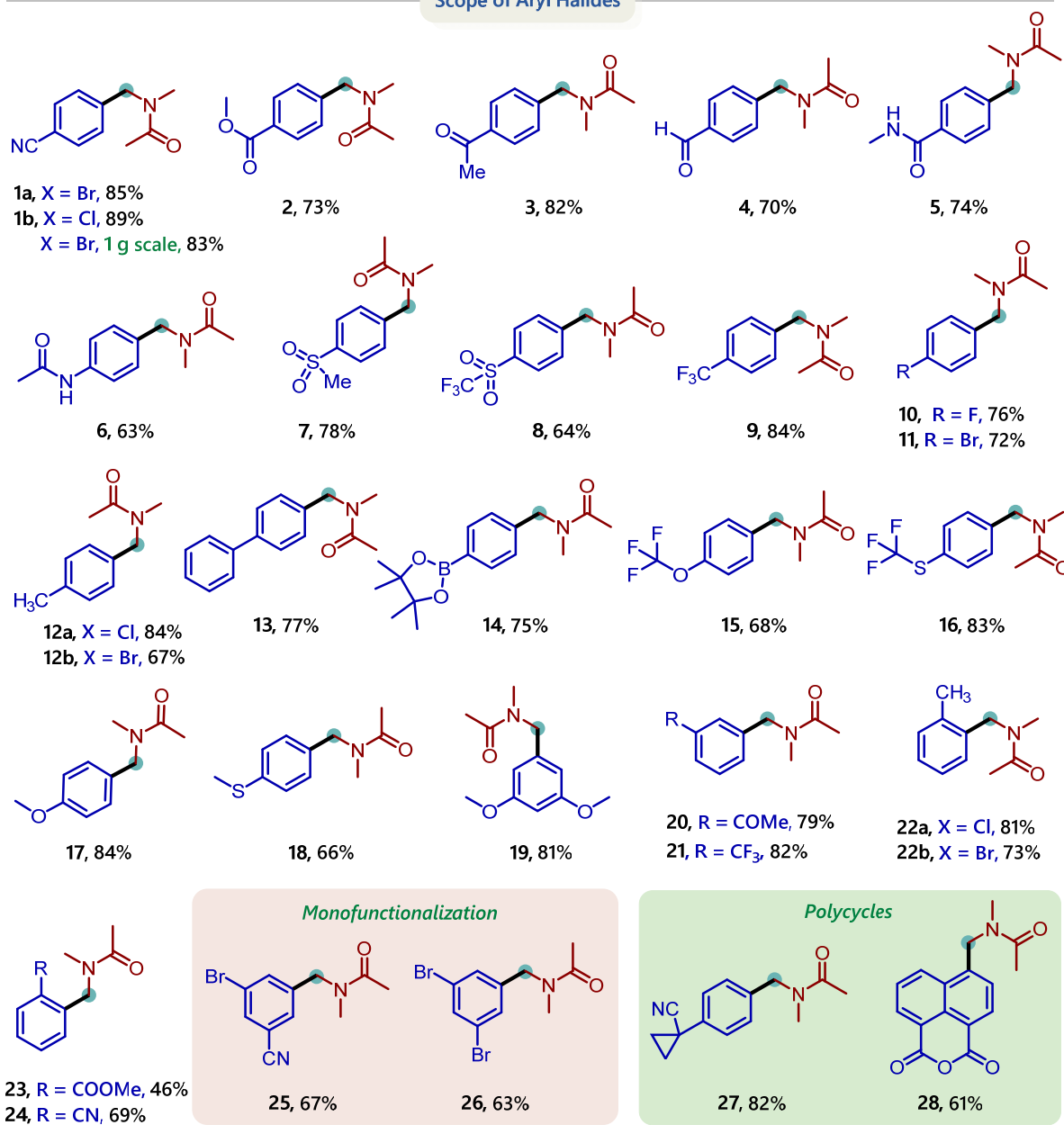


Fig. 2a | Scope of aryl halides. Yields of isolated products. Unless otherwise stated, products derive from their aryl bromide precursors.

amides (**5,6**), sulfone (**7**), trifluoromethyl sulfone (**8**) were tolerated. In addition, aryl boronic acid pinacol ester (**14**), and electrophilic sites that are sensitive to Ni-catalyzed cross coupling

reactions such as aryl halides (**10**, **11**) were also accommodated, thus providing handles for further functionalization. Aryl bromides, containing -CF₃ (**9**), -OCF₃ (**15**) or -SCF₃ (**16**) groups which are privileged functionalities in pharmaceuticals and agrochemicals, underwent arylation in good to excellent yields (68-84%). Moderately electron donating (**12b**) or electronically neutral (**13**) groups on the aryl moiety were well tolerated despite the propensity for homolytic C-H bond cleavage in the benzylic position of **12b**. In terms of the arene partner, the efficacy of the reaction was hardly impacted by either i) a change in electronic properties from *meta*-substitution (**20**, **21**) or ii) sterically encumbrance from *ortho*-substitution (**22b**, **23**, **24**). The reaction was very good compatible with highly electron rich aryl bromides among which the sulfide (**18**) or dimethoxy (**19**) containing moieties are particularly worth mentioning as they are generally considered to be labile towards oxidation by molecular photocatalysts. Gratifyingly, our method could be extended to aryl chlorides and **1b**, **12a** and **22a** were obtained in excellent yields (81-89%). Aryl moieties having more than one reactive site (**25**, **26**) are selectively mono-functionalized, thus allowing room for additional functionalization. The mpg-CN photochemical protocol was even effectively employed to polycyclic aryl bromides (**27**, **28**) in spite of their tendency for ring opening reaction in the presence of a nickel catalyst. Pleasingly, the developed conditions easily translated on a gram scale in batch-mode processing without noticeable erosion in yield (**1a**, 83%). Elsewhere, continuous flow chemistry is widely appreciated as an enabling technology for the scale-up of photochemical processes²³. Scalability was evaluated in two commercially-available suspension/slurry-handling continuous flow reactors (10-15 mL reactor sizes), one tubular reactor and one which used state-of-the-art oscillatory flow and pulsation technology together with hi-power LED modules (24-45 W radiant power). Surprisingly, preliminary results found conversion and productivity (mg h⁻¹) inferior to that obtained on gram-scale in a batch reactor (100 mL reactor size) and postulate that the mismatched time domains of a faster-flowing liquid phase and slower flowing solid particles in a continuously flowing stream is counter-productive for adsorption of reactive species to the mpg-CN surface in context of the photocatalytic chemistry herein (see the Supplementary Information for a detailed investigation).

Next, the amenability toward heteroaryl halides was assessed. Notably, our protocol displayed an exceptional level of tolerance towards a broad range of heteroaryl bromides as well as chlorides (**Fig. 2b**). A wide variety of electron-poor nitrogen-containing heterocycles such as pyridine (**33**), quinolines (**34**, **35**), isoquinoline (**36**), pyrimidine (**37**), indole (**38**), benzothiazole (**39**), thieno[2,3-*d*]pyrimidine (**40**) could all be functionalized. We note that such nitrogen-containing heterocycles bearing an amide functionality are typical scaffolds in many active

Scope of Hetero Aryl Halides

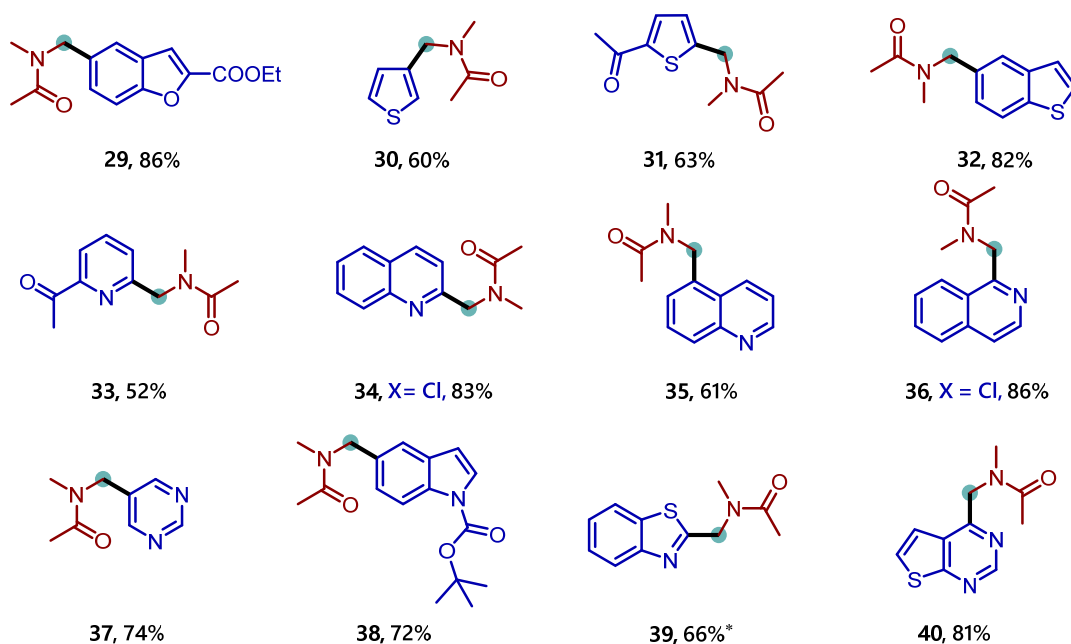


Fig 2b | Scope of heteroaryl halides. Yields of isolated products. Unless otherwise stated, products derive from their (hetero)aryl bromide precursors. *1.0 equivalent tetrabutylammonium chloride was used as an additive.

Scope of Naked Functionality

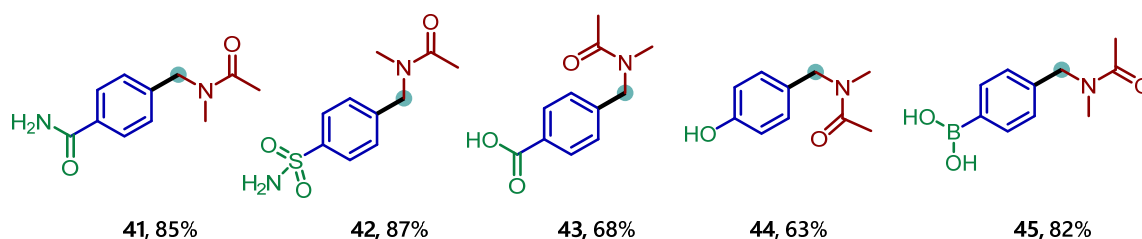


Fig. 2c | Scope of naked functional group tolerance. Yields of the isolated products. Unless otherwise stated, products derive from their aryl bromide precursors.

pharmaceutical ingredients. Moreover, electron-rich heterocycles such as benzofuran (**29**), thiophene (**30**, **31**) and benzothiophene (**32**) were also well tolerated. The robustness of mpg-CN photocatalysis compared to metallaphotoredox reactions of iridium polypyridyl complexes is a potential advantage. The iridium complexes could lead to lower product yields of electron-rich heterocycles due to the competing SET processes³¹. We then tested the compatibility of our mpg-CN photocatalytic arylation method with unprotected polar functional groups, an important criterion for assessing a method's robustness and applicability towards drug discovery and the synthesis of bioactive molecules. Strikingly, aryl bromides containing unprotected amide, sulfonamide, carboxylic acid, phenol or boronic acid functionalities all reacted smoothly and afforded the desired products (**41-45**) in excellent yields (**Fig. 2c**). For instance, the free -OH group in **44** remains untouched even though phenolic compounds are

typically sensitive towards oxidation under photochemical conditions. The presence of a boronic acid in **45** demonstrates i) the orthogonality of our protocol compared to classical metal-catalyzed cross-coupling reactions, and ii) our protocol's tolerance of a valuable handle for further synthetic transformations.

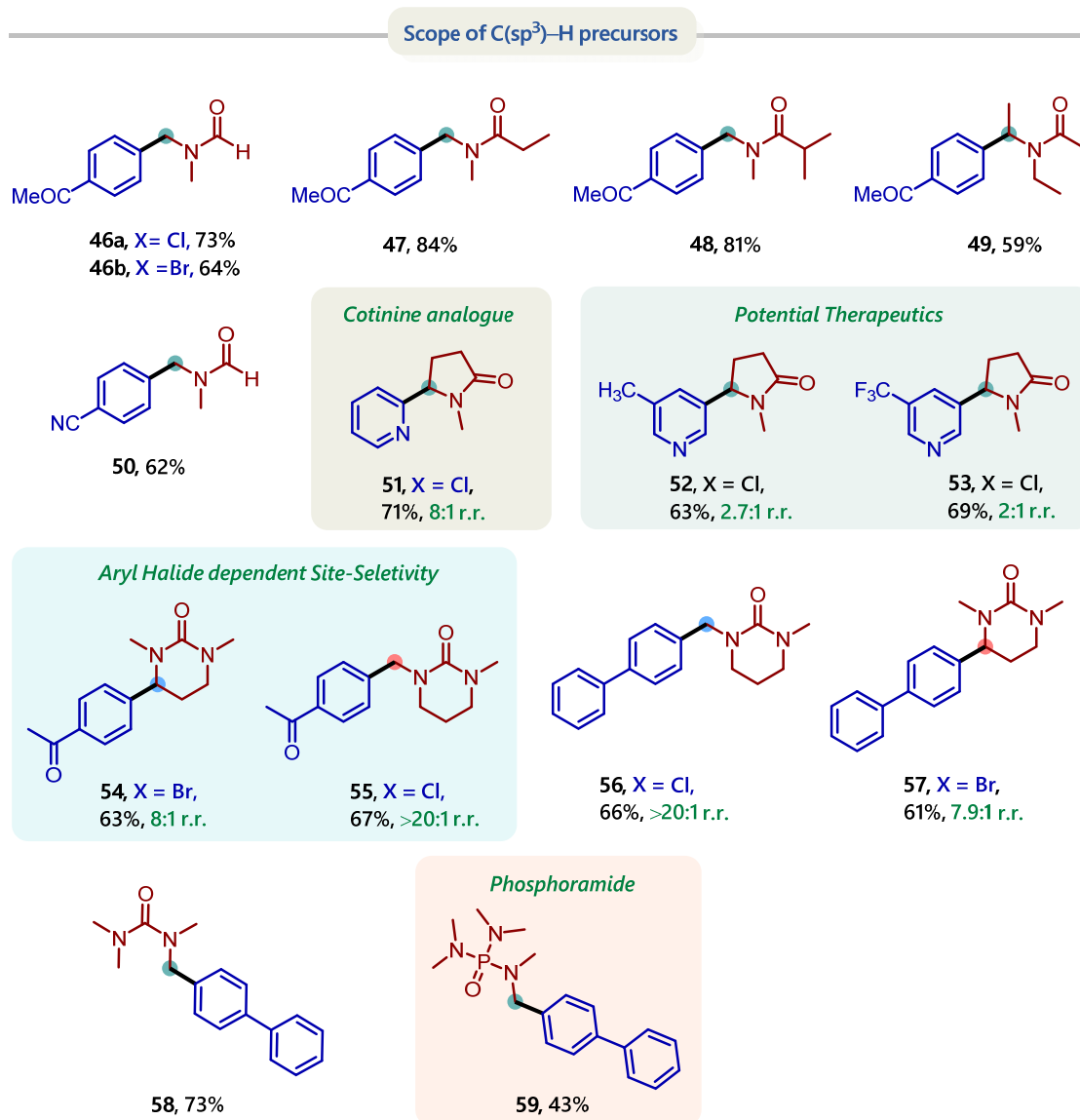


Fig: 3 | Scope of C(sp³)-H precursors. Yields of the isolated products. See the supporting information for aryl halide precursors. r.r. = regioisomeric ratio.

Encouraged by the aforementioned results, we expanded the mpg-CN semiconductor photocatalytic arylation method to C-H precursors other than DMA. Gratifyingly, this was possible, and a variety of acyclic and cyclic amides could be employed as C(sp³)-H bond functional handles with similar results to DMA. *N,N*-Dimethyl-formamide, -propionamide, -isobutyramide all furnished their corresponding arylated products (**46-48**, **50**) in good to excellent yields (73-84%). Even a more sterically encumbered secondary C(sp³)-H position of

N,N-diethyl acetamide (**49**) could be functionalized, albeit in slightly lower yields. Here it is worth mentioning that C–H arylation could also be performed in acetonitrile as solvent using 10 equivalents of amide C–H precursor and catalytic amounts of tetrabutylammonium chloride as an additive³². We were quite surprised to find that C(sp³)–H arylation of *N*-methyl pyrrolidone (NMP) with 2-chloropyridine rapidly afforded the corresponding Cotinine analogue (**51**) in very good yield and excellent regioselectivity. Although, 3-chloropyridine derivatives provided diminished regioselectivity, Cotinine **52**, the methyl analogue of a potential therapeutic agent against Alzheimer’s disease,³³ is not easily accessible by conventional synthetic methods and its –CF₃ derivative **53** has not been described. We observed high regioselectivity for methyl and methylene C–H bonds by choosing appropriate aryl halides. A cyclic urea derivative reacted preferentially at its *N*-CH₂ position in the presence of aryl bromides (**54**, **56**) whereas the same derivative reacted exclusively at its *N*-CH₃ position in the presence of aryl chlorides (**55**, **57**). This preference for activation of the least-substituted C–H bond by Cl radicals and activation of the most-substituted C–H bond by Br radicals reflects a previous report concerning C(sp³)–H functionalization of hydrocarbons²⁵. Interestingly, most of the compounds shown in **Fig. 3** have not been prepared before, illustrating the capability of our method to branch into new chemical space. For example, the successful arylation of hexamethylphosphoramide (**59**) as a C–H precursor provided rapid access to benzyl amine derivatives with potential physiological activity.

Post characterization of recovered mpg-CN. Apart from innate chemical and photostability, one of the prime advantages of mpg-CN is its heterogeneous nature that allows straightforward recovery of the catalyst from the reaction mixture, even from gram-scale reactions, employing simple centrifugation or filtration techniques. Moreover, the recovered catalyst can be reused multiple times preserving its photocatalytic reactivity. As demonstrated in the **Fig. 4a** mpg-CN photocatalyst can at least be recycled five times without appreciable loss in the product yield. The recovered material was characterized by a series of techniques used for the characterization of fresh mpg-CN (see the Supporting Information for details) such as Fourier-transform infrared spectroscopy (FT-IR), powder X-Ray diffraction (PXRD), X-ray photoelectron spectroscopy (XPS), X-Ray Analysis (EDX), energy dispersive inductively coupled plasma optical emission spectrometry (ICP-OES) transmission electron microscopy (TEM) etc.. The position and intensity of all peaks in FT-IR and PXRD spectrum revealed that the bulk chemical structure of the recovered photocatalyst was unchanged (**Fig. 4b**, **S13**), while EDX and XPS elemental analysis showed enhanced oxygen content on the surface of the recovered photocatalyst (Table S8 and S9). Additional, ICP-OES experiments identified 0.07±0.013 wt% Ni contained on the

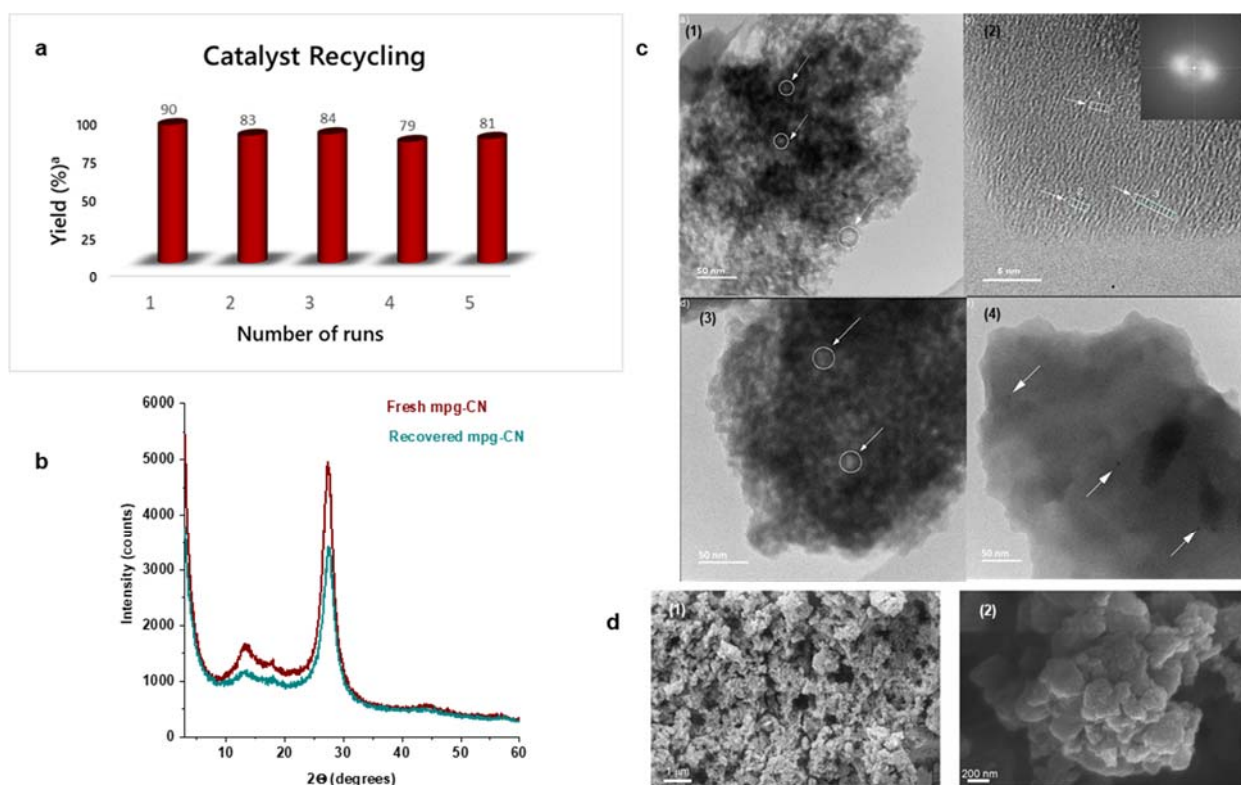


Fig. 4 | Characterization of fresh and recovered mpg-CN. **a**, Evaluation of catalytic recycling. **b**, PXRD pattern of fresh and recovered mpg-CN. **c**, TEM images of mpg-CN (1) fresh mpg-CN, overview image, circles mark mesopores, (2) HR-TEM image of fresh mpg-CN with the corresponding FFT as inset, (3) TEM image of recovered mpg-CN, overview image, circles mark mesopores, (4) TEM image of recovered mpg-CN, arrows indicate Ni(0) nanoparticles. **d**, SEM images of fresh mpg-CN (1) and recovered (2).

mpg-CN (Table S10). Interestingly, nickel 2p XPS did not show any distinct signal of nickel (**Fig. S23**). Considering that XPS is a surface-sensitive technique, such an apparently anomalous result confirmed that nickel in the sample is mainly located in the bulk of the material and completely removed from the surface. Similarly, no signal was observed in Br 3d XPS, which could potentially be related to using NiBr₂ as metal precursor (**Fig. S24**). HR-TEM images of the recovered mpg-CN i) indicated that its mesoporous structure was retained and ii) revealed the presence of dark spots with a diameter of 2-6 nm. These could be attributed to the formation of Ni(0) nanoparticles (**Fig. 4c**). Indeed, deposition of Ni(0) nanoparticles, albeit significantly larger amounts (1.4-12.6 wt.%) of Ni black, compared to ~0.07 wt.% in this work, has been previously reported^{34,35}. Nitrogen 1s XPS indicated the di-coordinated nitrogen of C=N-C moieties in tri-s-triazine unit as observed in the fresh catalyst (**Fig. S15**). The abundance of nitrogen atoms renders the material as an effective polydentate ligand to coordinate nickel atoms. Coordination with the covalent carbon nitride mpg-CN gives rise to a 16 electron Ni(II) chelate complex compared to a more reactive 14 electron Ni(II)-amide complex in the case of ionic carbon nitrides (**Fig. S25**). These observations indicate that the problem of nickel black formation in dual nickel/photoredox catalysis (in addition to adjusting the rates of oxidative

addition and reductive elimination by tuning the energy of incident light and the concentration of reagents)³⁴ could also be eliminated by using a robust carbon nitride photocatalyst stabilizes the low valent nickel species without altering the overall reaction rates. The recovered mpg-CN showed a slight shift of the absorption onset in the DRUV-vis spectrum and an expansion of the optical band gap by ~ 0.05 eV (**Fig. S19**). In steady-state PL such surface modification of mpg-CN is observed as a blue shift in fluorescence by ~ 0.1 eV (**Fig. S20**). The morphology of recovered mpg-CN particles adopted a more rounded shape compared to a rougher surface of freshly prepared mpg-CN (**Fig. 4d**). Taken together, the post characterization data of recovered mpg-CN clearly shows robustness, stability and durability of this heterogeneous organic semiconductor as a photocatalyst.

Mechanistic investigation. The aforementioned results provide evidence for catalytic generation of HAT agent on the mpg-CN semiconductor surface, which operates in synergy with nickel catalysis to enable $C(sp^3)$ –H bond functionalization. However, the photoactivity of mpg-CN/nickel dual catalytic system for C–H bond cleavage at a molecular level remains to be elucidated. Based on prior mechanistic investigations of photo/Ni-dual catalyzed cross coupling reactions in homogeneous systems^{32,36,37}, we postulate two plausible mechanistic scenarios as depicted in **Fig. 5**. Initially, the Ni(0) complex **I** undergoes oxidative addition with an aryl halide delivering Ni(II) oxidative addition complex **II**. Concurrently, light absorption by the mpg-CN semiconductor photocatalyst triggers the charge separation producing two-dimensional surface redox centres as electron–hole pairs.

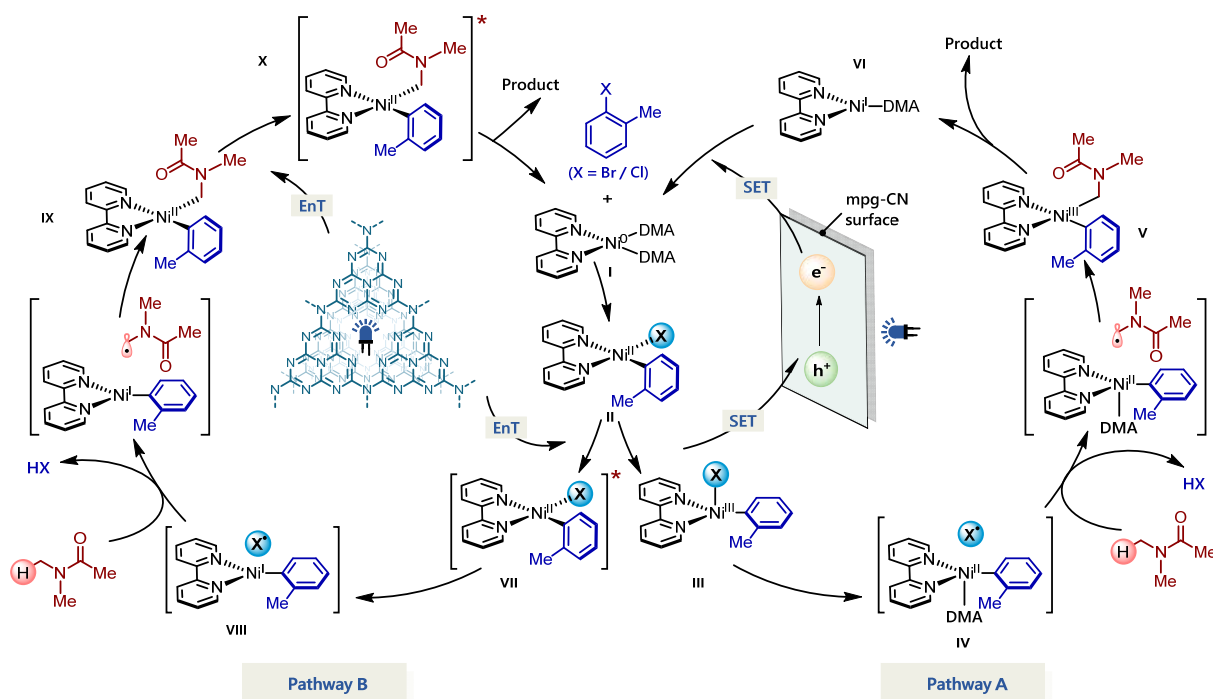


Fig. 5 | Plausible mechanistic pathways for mpg-CN/nickel photocatalytic $C(sp^3)$ –H arylation.

In pathway A, SET oxidation of complex **II** by the photogenerated hole (VBM located at +1.2 V vs SCE, $E_{1/2}(\text{Ni}^{\text{II}}/\text{Ni}^{\text{III}}) = +0.85$ V vs SCE) affords species **III**³¹, which may undergo Ni(III)–X homolysis to give a halogen radical and Ni(II) species **IV**³⁸. The resulting halogen radical can rapidly abstract a hydrogen atom from DMA (H–Br BDE ~88 kcal/mol, H–Cl BDE ~102 kcal/mol, α -amino C–H BDE ~89 to 94 kcal/mol)²⁸ which immediately recombines with species **IV** to form **V**. Subsequent reductive elimination of **V** results in the desired product and Ni(I) species **VI**. Finally, reduction of **VI** by the electron located on the semiconductor surface (CBM located at –1.5 V vs SCE, $E_{1/2}(\text{Ni}^{\text{I}}/\text{Ni}^0) = -1.42$ V vs SCE)³⁶ regenerates Ni(0) and completes the catalytic cycle. In pathway B, mpg-CN serves as a light absorbing antenna undergoing an energy transfer process (EnT) (singlet-triplet band gap *ca.* 0.39 eV)³⁹ to produce electronically excited Ni(II) species **VII**. Homolysis of the Ni(II)–X bond and HAT followed by rebound of the resulting carbon centered radical with **VIII** generates Ni(II) species **IX**⁴⁰. Reductive elimination from the electronically excited species **X**, promoted by EnT with mpg-CN, provides the final product and regenerates Ni(0) species thus completing the catalytic cycle. Control experiments (Table S11) with a catalytic amount of preformed [(bpy)Ni^{II}(*o*-tolyl)Br] complex **II** in our standard reaction conditions show that both complex **II** and mpg-CN are required in the productive reaction pathway. A major distinction between these two pathways as shown in **Fig. 5** is that EnT process involves the excited state of Ni(II) species which should be directly accessible via visible light excitation in the absence of photocatalyst (**Fig. S26**). Indeed, a stoichiometric experiment with [(bpy)Ni^{II}(*o*-tolyl)Br] complex **II** *via* direct photoexcitation at 450 nm (*i.e.* without mpg-CN) revealed the formation of the desired product in appreciable yield (Table S12). An additional control experiment performed under identical conditions in the absence of light failed to produce any detectable product. These experiments are indicative towards pathway B where the formation of an electronically excited Ni(II) complex is a prerequisite for bond formation. Pseudo-zero order and zero-order kinetic behaviour were also observed during time-course experiments³⁷ (see the Supplementary Information). Nevertheless, we cannot rule out the possibility of a disproportionation reaction between photoexcited Ni(II)* and ground state Ni(II) to give Ni(I) and Ni(III) species followed by reductive elimination to afford the product. However, the low concentration as well as short lifetime of the Ni(II)* complex (*ca.* $\tau = 2.53$ ns for [(bpy)Ni^{II}(*o*-tolyl)Br]) make this mechanism very unlikely to be a major contributing pathway⁴¹.

Application in the synthesis of bio-active molecules. Finally, we demonstrated the application of our mpg-CN photocatalytic C(sp³)–H arylation method to the late-stage functionalization of bio-active molecules including pharmaceuticals, hormones, agrochemicals (pesticide,

fungicide) as aryl coupling components and were delighted to observe desired products (**60-74**) in good to excellent yields. Our protocol therefore enlarges the palette of opportunities for modern applications in drug discovery and agrochemicals.

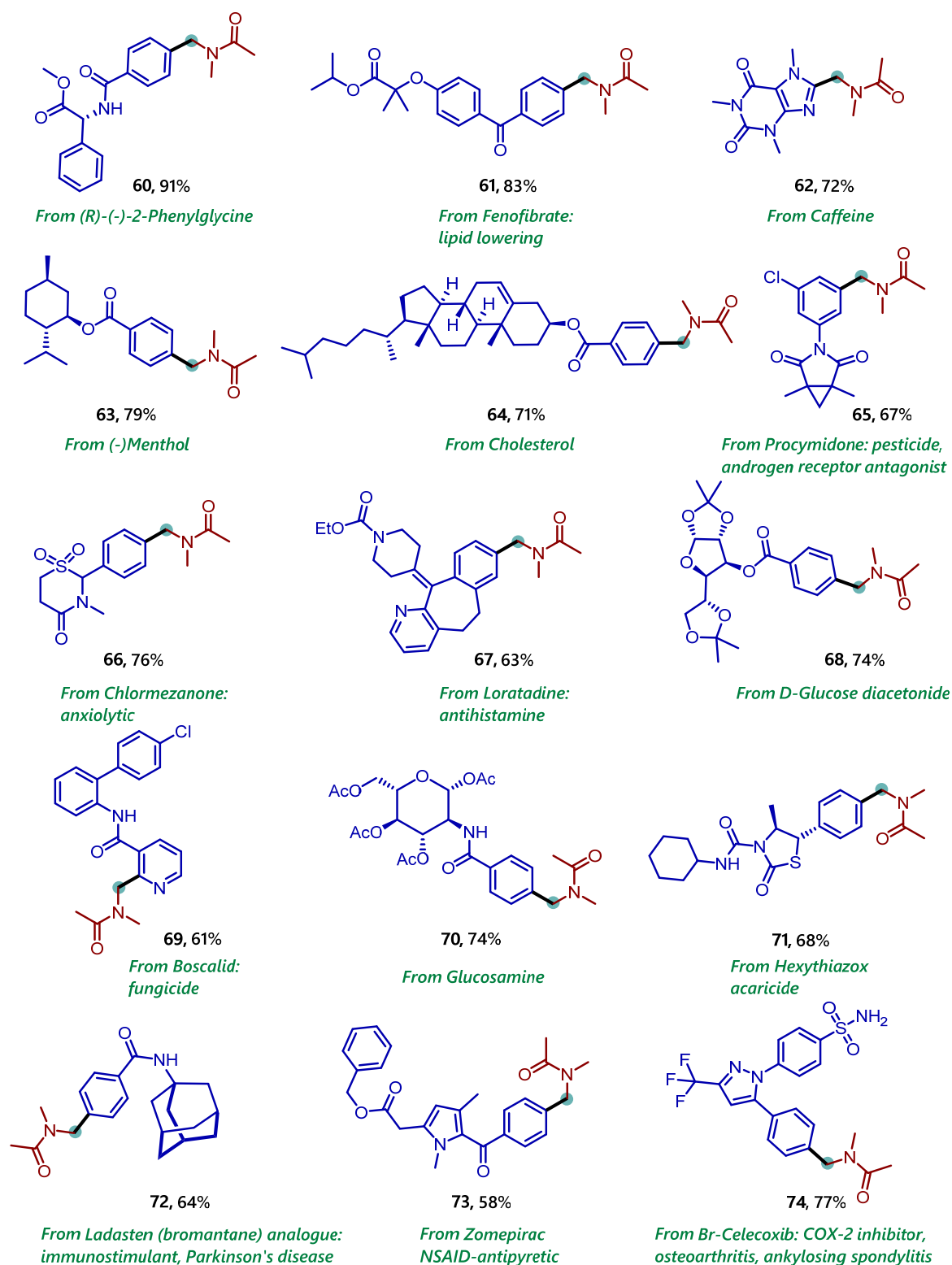


Fig. 6 | Application of the mpg-CN photocatalytic C(sp³)-H arylation method to bio-active molecules. See the supporting information for (hetero)aryl halide precursors.

Conclusion

We have demonstrated the so far unrecognized potential of mesoporous graphitic carbon nitride (mpg-CN) in direct (hetero)arylations of C(sp³)-H bonds *via* a synergistic combination with nickel catalysis. Catalytically-generated halogen radicals act as hydrogen atom transfer agents for the functionalization of C(sp³)-H bonds, while tolerating a large number of functional groups. The protocol, based on a durable organic semiconductor mpg-CN photocatalyst and a simple nickel catalyst, provides a powerful alternative to conventional homogeneous photoredox catalysts. From a sustainable chemistry perspective, our protocol offers a distinct advantage over others. Namely, its heterogeneous nature means that mpg-CN is readily recovered from the reaction media by simple centrifugation and can be reused multiple times without appreciable loss in activity. Gram-scale reactions are possible in batch, where batch-processing surprisingly provided a more viable option for scale-up than continuous flow using a dedicated slurry-handling oscillatory flow reactors. Mechanistic investigations provide evidence of an energy transfer driven pathway generating an electronically excited nickel complex as a reactive intermediate. Lastly, the potentiality of mpg-CN as an attractive visible light absorbing organic semiconductor photocatalyst has been manifested by performing late-stage functionalization on complex molecules. Considering the use of bio-active (hetero)aromatic halides as potential coupling partners, the cost-effective technology may find applications in modern drug discovery. Finally, we believe that the distinct reactivity mode of mpg-CN described herein may lead novel designs in EnT catalysis.

References

1. Yoon, T. P., Ischay, M. A. & Du, J. Visible light photocatalysis as a greener approach to photochemical synthesis. *Nat. Chem.* **2**, 527-532 (2010).
2. Marzo, L., Pagire, S. K., Reiser, O. & König, B. Visible-Light Photocatalysis: Does It Make a Difference in Organic Synthesis? *Angew. Chem. Int. Ed.* **57**, 10034-10072 (2018).
3. Stephenson, C. & Yoon, T. P. Enabling Chemical Synthesis with Visible Light. *Acc. Chem. Res.* **49**, 2059-2060 (2016).
4. Cernak, T., Dykstra, K. D., Tyagarajan, S., Vachal, P. & Krska, S. W. The medicinal chemist's toolbox for late stage functionalization of drug-like molecules. *Chem. Soc. Rev.* **45**, 546-576 (2016).
5. Liao, K. *et al.* Site-selective and stereoselective functionalization of non-activated tertiary C-H bonds. *Nature* **551**, 609-613 (2017).
6. Shaw, M. H., Twilton, J. & MacMillan, D. W. C. Photoredox Catalysis in Organic Chemistry. *J. Org. Chem.* **81**, 6898-6926 (2016).
7. Romero, N. A. & Nicewicz, D. A. Organic Photoredox Catalysis. *Chem. Rev.* **116**, 10075-10166 (2016).
8. Kisch, H. Semiconductor Photocatalysis—Mechanistic and Synthetic Aspects. *Angew. Chem. Int. Ed.* **52**, 812-847 (2013).
9. Devery Iii, J. J. *et al.* Ligand functionalization as a deactivation pathway in a *fac*-Ir(ppy)₃-mediated radical addition. *Chem. Sci.* **6**, 537-541 (2015).
10. O'Brien, C. J. *et al.* Photoredox Cyanomethylation of Indoles: Catalyst Modification and Mechanism. *J. Org. Chem.* **83**, 8926-8935 (2018).
11. Ghosh, I. *et al.* Organic semiconductor photocatalyst can bifunctionalize arenes and heteroarenes. *Science* **365**, 360 (2019).

12. Majek, M., Filace, F. & Wangelin, A. J. v. On the mechanism of photocatalytic reactions with eosin Y. *Beilstein J. Org. Chem.* **10**, 981-989 (2014).
13. Wang, X. *et al.* A metal-free polymeric photocatalyst for hydrogen production from water under visible light. *Nat. Mater.* **8**, 76-80 (2009).
14. Wang, Y., Wang, X. & Antonietti, M. Polymeric Graphitic Carbon Nitride as a Heterogeneous Organocatalyst: From Photochemistry to Multipurpose Catalysis to Sustainable Chemistry. *Angew. Chem. Int. Ed.* **51**, 68-89 (2012).
15. Liebig, J. Über einige Stickstoff - Verbindungen. *Ann. Pharm.* **10**, 1-47 (1834).
16. Savateev, A., Ghosh, I., König, B. & Antonietti, M. Photoredox Catalytic Organic Transformations using Heterogeneous Carbon Nitrides. *Angew. Chem. Int. Ed.* **57**, 15936-15947 (2018).
17. Gerwien, A., Schildhauer, M., Thumser, S., Mayer, P. & Dube, H. Direct evidence for hula twist and single-bond rotation photoproducts. *Nat. Commun.* **9**, 2510 (2018).
18. Lin, J., Pan, Z. & Wang, X. Photochemical Reduction of CO₂ by Graphitic Carbon Nitride Polymers. *ACS Sustain. Chem. Eng.* **2**, 353-358 (2014).
19. Caputo, C. A. *et al.* Photocatalytic Hydrogen Production using Polymeric Carbon Nitride with a Hydrogenase and a Bioinspired Synthetic Ni Catalyst. *Angew. Chem. Int. Ed.* **53**, 11538-11542 (2014).
20. Capaldo, L. & Ravelli, D. Hydrogen Atom Transfer (HAT): A Versatile Strategy for Substrate Activation in Photocatalyzed Organic Synthesis. *Eur. J. Org. Chem.* **2017**, 2056-2071 (2017).
21. Cai, Y. *et al.* Heterogeneous Visible-Light Photoredox Catalysis with Graphitic Carbon Nitride for α -Aminoalkyl Radical Additions, Allylations, and Heteroarylations. *ACS Catal.* **8**, 9471-9476 (2018).
22. Deng, H.-P., Fan, X.-Z., Chen, Z.-H., Xu, Q.-H. & Wu, J. Photoinduced Nickel-Catalyzed Chemo- and Regioselective Hydroalkylation of Internal Alkynes with Ether and Amide α -Hetero C(sp³)-H Bonds. *J. Am. Chem. Soc.* **139**, 13579-13584 (2017).
23. Laudadio, G. *et al.* C(sp³)-H functionalizations of light hydrocarbons using decatungstate photocatalysis in flow. *Science* **369**, 92 (2020).
24. Ruffoni, A. *et al.* Practical and regioselective amination of arenes using alkyl amines. *Nat. Chem.* **11**, 426-433 (2019).
25. Jia, P. *et al.* Light-Promoted Bromine-Radical-Mediated Selective Alkylation and Amination of Unactivated C(sp³)-H Bonds. *Chem* **6**, 1766-1776 (2020).
26. Choi, G. J., Zhu, Q., Miller, D. C., Gu, C. J. & Knowles, R. R. Catalytic alkylation of remote C-H bonds enabled by proton-coupled electron transfer. *Nature* **539**, 268-271 (2016).
27. Chu, J. C. K. & Rovis, T. Amide-directed photoredox-catalysed C-C bond formation at unactivated sp³ C-H bonds. *Nature* **539**, 272-275 (2016).
28. Shaw, M. H., Shurtleff, V. W., Terrett, J. A., Cuthbertson, J. D. & MacMillan, D. W. C. Native functionality in triple catalytic cross-coupling: sp³ C-H bonds as latent nucleophiles. *Science* **352**, 1304-1308 (2016).
29. Strieth-Kalthoff, F., James, M. J., Teders, M., Pitzer, L. & Glorius, F. Energy transfer catalysis mediated by visible light: principles, applications, directions. *Chem. Soc. Rev.* **47**, 7190-7202 (2018).
30. Beyreuther, B. K. *et al.* Lacosamide: A Review of Preclinical Properties. *CNS Drug Rev.* **13**, 21-42 (2007).
31. Shields, B. J. & Doyle, A. G. Direct C(sp³)-H Cross Coupling Enabled by Catalytic Generation of Chlorine Radicals. *J. Am. Chem. Soc.* **138**, 12719-12722 (2016).
32. Rohe, S., Morris, A. O., McCallum, T. & Barriault, L. Hydrogen Atom Transfer Reactions via Photoredox Catalyzed Chlorine Atom Generation. *Angew. Chem. Int. Ed.* **57**, 15664-15669 (2018).
33. Echeverria, V. & Zeitlin, R. Cotinine: a potential new therapeutic agent against Alzheimer's disease. *CNS Neurosci. Ther.* **18**, 517-523 (2012).
34. Gisbertz, S., Reischauer, S. & Pieber, B. Overcoming limitations in dual photoredox/nickel-catalysed C-N cross-couplings due to catalyst deactivation. *Nat. Catal.* **3**, 611-620 (2020).
35. Pieber, B. *et al.* Semi-heterogeneous Dual Nickel/Photocatalysis using Carbon Nitrides: Esterification of Carboxylic Acids with Aryl Halides. *Angew. Chem. Int. Ed.* **58**, 9575-9580 (2019).
36. Diccianni, J. B. & Diao, T. Mechanisms of Nickel-Catalyzed Cross-Coupling Reactions. *Trends Chem.* **1**, 830-844 (2019).
37. Malik, J. A., Madani, A., Pieber, B. & Seeberger, P. H. Evidence for Photocatalyst Involvement in Oxidative Additions of Nickel-Catalyzed Carboxylate *O*-Arylations. *J. Am. Chem. Soc.* **142**, 11042-11049 (2020).
38. Hwang, S. J. *et al.* Halogen Photoelimination from Monomeric Nickel(III) Complexes Enabled by the Secondary Coordination Sphere. *Organometallics* **34**, 4766-4774 (2015).
39. Savateev, A. *et al.* Potassium Poly(Heptazine Imide): Transition Metal-Free Solid-State Triplet Sensitizer in Cascade Energy Transfer and [3+2]-cycloadditions. *Angew. Chem. Int. Ed.* **59**, 15061-15068 (2020).
40. Heitz, D. R., Tellis, J. C. & Molander, G. A. Photochemical Nickel-Catalyzed C-H Arylation: Synthetic Scope and Mechanistic Investigations. *J. Am. Chem. Soc.* **138**, 12715-12718 (2016).

41. Welin, E. R., Le, C., Arias-Rotondo, D. M., McCusker, J. K. & MacMillan, D. W. C. Photosensitized, energy transfer-mediated organometallic catalysis through electronically excited nickel(II). *Science* **355**, 380-385 (2017).

Acknowledgements

The German Science Foundation (DFG, KO 1537/18-1) supported this work. This project has received funding from the European Research Council (ERC) under the European Union's Horizon 2020 Research and Innovation Programme (grant agreement No. 741623). We thank Dr. Rudolf Vasold for GC-MS measurements and Regina Hoheisel for Cyclic Voltammetry measurements. We also thank Miss Jiamei Liu at Instrument Analysis Center of Xi'an Jiaotong University for her assistance with XPS analysis and Bolortuya Badamdorj for acquiring TEM images. We thank Dr. Hannes Gemoets for helpful discussions and CreaFlow for providing an oscillatory flow reactor (HANU reactor) and Peschl Ultraviolet GmbH for providing an appropriate hi-power LED module.

Author contributions

B.K. guided the research. B.K. and S.D. conceived and designed the project. S.D. and B.K. wrote the manuscript, with input from others. S.D., K.M. and G.V.R. performed and analyzed the experiments. J.K. and J.B. collaborated with S.D. to investigate scale-up options in continuous flow systems and collected time-course data. M.A. and A.S. provided the mpg-CN and characterised the fresh and recovered photocatalyst. All authors discussed the results and commented on the manuscript.

Competing interests

The authors declare no conflicts of interest.